

A Hot Water Bottle for Aging Neutron Stars

Mark Alford,¹ Pooja Jotwani,² Chris Kouvaris,³ Joydip Kundu,⁴ and Krishna Rajagopal³

¹*Physics Department, Washington University, St. Louis, MO 63130, USA*

²*Charles W. Flanagan High School, Pembroke Pines, FL 33029, USA*

³*Center for Theoretical Physics, Massachusetts Institute of Technology, Cambridge, MA 02139, USA*

⁴*Department of Physics, University of Maryland, College Park, MD 20742, USA*

(Dated: November, 2004)

The gapless color-flavor locked (gCFL) phase is the second-densest phase of matter in the QCD phase diagram, making it a plausible constituent of the core of neutron stars. We show that even a relatively small region of gCFL matter in a star will dominate both the heat capacity C_V and the heat loss by neutrino emission L_ν . The gCFL phase is characterized by an unusual quasiparticle dispersion relation that makes both its specific heat c_V and its neutrino emissivity ε_ν parametrically larger than in any other phase of nuclear or quark matter. During the epoch in which the cooling of the star is dominated by direct Urca neutrino emission, the presence of a gCFL region does not strongly alter the cooling history because the enhancements of C_V and L_ν cancel against each other. At late times, however, the cooling is dominated by photon emission from the surface, so L_ν is irrelevant, and the anomalously large heat capacity of the gCFL region keeps the star warm. The temperature drops with time as $T \sim t^{-1.4}$ rather than the canonical $T \sim t^{-5}$. This provides a unique and potentially observable signature of gCFL quark matter.

PACS numbers: Valid PACS appear here

I. INTRODUCTION

It has often been suggested that the core of a neutron star may contain quark matter in one of the color-superconducting phases [1]. The densest predicted phase on the QCD phase diagram is the color-flavor locked (CFL) phase, which is a color superconductor but an electromagnetic insulator [1, 2]. The second-densest phase is the gapless CFL (gCFL) phase, which is a conductor with a nonzero density of electrons [3, 4, 5, 6]. It also has gapless quark quasiparticles, one of which has an almost-quadratic dispersion relation, arising without fine-tuning because it is enforced by the requirement that the matter be electrically neutral [3, 4]. We show in this paper that this characteristic feature of the gCFL phase means that if quark matter in this phase is present in a neutron star, it dominates the heat capacity and neutrino luminosity, and therefore controls the cooling of the star. At late times this produces a unique signature, as the large heat capacity keeps the star anomalously warm. A neutron star that is tens of millions of years old will be an order of magnitude or more warmer if it contains a region of gCFL quark matter than if it does not.

In any speculation about the phases of matter that occur inside a neutron star, the main challenge is to provide observable signatures of the presence of these phases. Since we are proposing such a signature, albeit one that presents significant observational challenges, we first set the stage with a quick survey of previous proposals.

- **Mass-radius relation.** If we could measure the mass and radius of several neutron stars to a reasonable accuracy, mapping out the mass-radius relationship, we would have a strong constraint on the equation of state of dense matter. However, although such measurements would dramatically reduce the current uncertainties in our knowl-

edge of the equation of state of the nuclear matter “mantle” of neutron stars, and could yield evidence of some sort of exotic phase in the core, they would not provide specific evidence of the presence of quark matter [7, 8].

- **Double pulsar timing.** There is a good prospect that the long term analysis of the recently discovered binary double pulsar [9] may yield a measurement of the moment of inertia of a neutron star [10]. This would provide information about the density profile that is complementary to that obtained from a mass-radius relation, as it would constrain the “compactness” of a star.

- **Gravitational waves from collisions.** If we could detect gravity waves from neutron stars spiraling into black holes in binary systems, we could perhaps analyze them for information about the density profile of the neutron star, in particular the presence of an interface separating a denser quark core from a less-dense nuclear mantle [11].

- **Spinning out a quark matter core.** If conditions are “just so”, rapidly spinning oblate neutron stars may not have quark matter in their cores even though more slowly rotating spherical neutron stars do. This could be detected either by anomalies in braking indices of stars that are “spinning down” [12] or by anomalous population statistics of stars that are being “spun up” by accretion [13]. Recent observations show no sign of such an effect in the histogram of spin-frequencies of stars in the act of being spun up [14], indicating that if quark matter is present, spinning the star and making it oblate does not get rid of it. If there is a quark matter core, it must therefore occupy a reasonable fraction of the star.

- **r -modes.** A rapidly spinning neutron star will quickly slow down if it is unstable with respect to bulk flows known as r -modes, which transfer the star’s angular momentum into gravitational radiation. This phenomenon will only occur if damping is sufficiently small, so it pro-

vides a probe of the viscosity of the interior of the star. Such arguments have been used to rule out the possibility that pulsars are made entirely of CFL quark matter [15], in which viscous damping is negligible [15, 16], but their implications for the possibility of CFL quark matter localized within the core of a neutron star have not yet been analyzed. Since gCFL quark matter is expected to have a large viscosity, its presence is unlikely to be constrained by r -mode arguments.

- **Core glitches.** If the third-densest phase on the QCD phase diagram is not nuclear matter, it must be a form of quark matter with less pairing than in the gCFL phase. A leading candidate is the crystalline color superconducting phase [17]. If this form of quark matter occurs within the core of a neutron star, because it is both superfluid and crystalline it may be a locus for pulsar glitches. This proposal has not yet been worked out sufficiently quantitatively to determine whether such core glitches are observable and if so whether they are consistent with (some) observed glitches.

- **Direct neutrino detection.** Neutrinos have a long mean free path even in nuclear matter, so they can potentially carry information about the core directly to the outside world. Not coincidentally, neutrinos are very hard to detect, and the only time when a neutron star emits enough neutrinos to be detectable on earth is during the first few seconds after the supernova explosion. The time-of-arrival distribution of supernova neutrinos could teach us about possible phase transitions to and in quark matter [18, 19], but analysis of this proposal requires a better understanding of both the supernova itself and of the properties of quark matter at MeV temperatures, where the phase diagram of QCD is more baroque than at zero temperature [5, 6].

- **Cooling.** A much better prospect is the indirect detection of neutrino emission, which is the dominant heat loss mechanism for the first million years or so, and can therefore be inferred from measurements of neutron star temperature as a function of age. Moreover, because both neutrino emission rates and heat capacity generally rise with density, neutron star cooling is likely to be preferentially sensitive to the properties of matter in the core of a neutron star.

The qualitative distinction among cooling behaviors that may be discerned from the measurement of temperatures of stars that are 10^{3-6} years old is between stars in which direct Urca processes are allowed (which yields a neutrino emissivity $\varepsilon_\nu \sim T^6$), leading to rapid cooling, and stars in which direct Urca processes are forbidden [7, 20, 21, 22, 23, 24]. Ordinary nuclear matter is unusual in that its direct Urca processes $n \rightarrow p + e + \bar{\nu}$ and $p + e \rightarrow n + \nu$ are kinematically forbidden, meaning that neutrino emission relies upon slower reactions ($\varepsilon_\nu \sim T^8$). Direct Urca processes are allowed in sufficiently dense nuclear matter, nuclear matter with nonzero hyperon density [25], pion condensation [26] or kaon condensation [27], and in all proposed phases of quark matter except CFL [28]. In the CFL phase, there are no direct

Urca processes because thermally excited quark quasiparticles are exponentially rare. There are neutrino emission processes involving collective excitations that lead to $\varepsilon_\nu \sim T^{15}$ [19], but in reality any CFL quark matter within a star will cool by conduction, not by neutrino emission [29]. Indeed, because all forms of dense matter are good heat conductors the cooling of a star tends to be dominated by whichever phase has the highest neutrino emissivity. Hence, the discovery of fast cooling would only tell us that some part of the star consists of one of the many phases that allow direct Urca. Discovery of stars that cool slowly would be an indication that they contain only medium-density nuclear matter and perhaps CFL quark matter.

To date, none of the schemes listed above has provided an unambiguous signature of the presence of quark matter, although all are the subject of ongoing observational effort, which in turn drives improvements on the theoretical side. In this paper, we argue that recent theoretical advances in our understanding of the properties of quark matter offer the prospect of an unambiguous detection, if it is possible to measure the temperatures of neutron stars that are old enough that their cooling is no longer dominated by neutrino emission. Admittedly, this presents an observational challenge. However, it is a challenge that has not been closely studied prior to our work, since all forms of dense matter *except* gCFL quark matter result in neutron stars that cool comparably (and very) rapidly in their old age. We show that quark matter in the gCFL phase keeps aged neutron stars (those significantly older than a million years) much warmer than is predicted by any other assumed dense matter physics.

Younger neutron stars containing gCFL quark matter have a faster-than-standard direct Urca neutrino emissivity $\varepsilon_\nu \sim T^{5.5}$, but this does not lead to faster-than-standard-direct-Urca cooling because of the correspondingly enhanced gCFL specific heat.

In Section II, we introduce the relevant properties of the gapless CFL phase of quark matter, and in Sections III and IV we present the calculations of its specific heat c_V and neutrino emissivity ε_ν , respectively. These are our central calculational results. We do not provide a state-of-the-art calculation of the cooling of a neutron star containing gCFL quark matter. Instead, in Section V, we provide an introduction to the physics of neutron star cooling that suffices to illustrate the qualitative consequences of the quantitative results for the gCFL c_V and ε_ν . The astrophysically inclined reader interested in our results and their implications but not in their derivation can find c_V in Eq. (8) and ε_ν in (31) and, more conveniently, Fig. 2 and should read the text around these results and then turn to Section V.

II. INTRODUCTION TO THE GAPLESS CFL PHASE OF QUARK MATTER

At any densities that are high enough that nucleons are crushed into quark matter, the quark matter that results at sufficiently low temperatures is expected to be in one of a family of color superconducting phases, with Cooper pairing of quarks near their Fermi surfaces [1]. The QCD quark-quark interaction is strong and is attractive between quarks that are antisymmetric in color. If there is quark matter in the cores of neutron stars, we therefore expect it to be color superconducting. The phenomenon persists to asymptotically high densities, where the interaction becomes weak and *ab initio* calculations of properties of color superconducting matter become rigorous [1]. The QCD phase diagram exhibits a rich structure of color superconducting phases as a function of temperature and density [1, 5, 6], but in this paper we can simplify it by working at zero temperature. This is reasonable because we will be discussing neutron stars with temperatures in the keV range, which is orders of magnitude colder than the various critical temperatures at which phase transitions between different quark matter phases occur.

A. The CFL phase under stress

At asymptotically high densities, where the up, down and strange quarks can be treated on an equal footing and the disruptive effects of the strange quark mass can be neglected, quark matter is in the color-flavor locked (CFL) phase, in which quarks of all three colors and all three flavors form Cooper pairs [2]. The CFL phase is a color superconductor but is an electromagnetic insulator, with zero electron density. In real-world quark matter, as may exist in the cores of compact stars, the density is not asymptotically high. The quark chemical potential μ is of order 500 MeV at most, making it important to include the effects of the strange quark mass M_s , which is expected to be density dependent, lying somewhere between the current mass ~ 100 MeV and the vacuum constituent quark mass ~ 500 MeV. To describe macroscopic regions of quark matter, we must also impose electromagnetic and color neutrality [30, 31, 32] and allow for equilibration under the weak interactions. The CFL pairing pattern is antisymmetric in flavor, color, and spin, so it involves pairing between different flavors. For this reason, the effect of a relatively large M_s , combined with weak equilibration and the neutrality constraints, is to put a stress on the CFL pairing pattern: these effects would all act to pull apart the Fermi momenta of the different flavors by an amount of order M_s^2/μ in the absence of CFL pairing. (This can be seen by an analysis of neutral unpaired quark matter in which the Fermi momenta of the d , u and s quarks are split by $\simeq M_s^2/4\mu$.) In the CFL phase, Fermi momenta do not separate [33] but the consequence of the stress is that the excitation energies of those fermionic quasiparticles

whose excitation would serve to ease the stress by breaking pairs and separating Fermi surfaces is reduced, again by of order M_s^2/μ [3]. When the density becomes low enough, some of the quasiparticles become gapless, the CFL pairing pattern is disrupted, and we enter the gapless CFL (gCFL) phase [3, 4], the second-densest phase on the QCD phase diagram. Since the strength of the CFL pairing is measured by the gap parameter Δ_{CFL} , and the stress on it is of order M_s^2/μ , the CFL pattern “breaks” and the CFL→gCFL transition occurs when the density is low enough that $M_s^2/\mu \sim \Delta_{CFL}$. Making this argument quantitative results in the prediction of a $T = 0$ second-order insulator-metal transition separating the CFL and gCFL phases at $M_s^2/\mu \simeq 2\Delta_{CFL}$ [3, 4]. An analogous zero temperature metal insulator transition has been analyzed in Ref. [34]. (If the CFL phase is augmented by a K^0 -condensate [35, 36], the CFL→gCFL transition is delayed to a value of M_s^2/μ that is higher by a factor of 4/3 [37] or less [36].)

B. The nature of gCFL pairing

In the gCFL phase the pairing is still antisymmetric in flavor as well as color and spin, so as in CFL there are diquark condensates (gap parameters) $\Delta_1 \sim \langle ds \rangle$, $\Delta_2 \sim \langle us \rangle$, $\Delta_3 \sim \langle ud \rangle$. But unlike the CFL phase, where the gap parameters are very similar, $\Delta_1 = \Delta_2 \simeq \Delta_3$, in gCFL the pairing involving strange quarks is suppressed: very strongly for $\langle ds \rangle$, and quite strongly for $\langle us \rangle$, so that $\Delta_1 < \Delta_2 < \Delta_3$, as shown in Figures in Refs. [3, 4, 6]. The result is that while quarks of all three colors and all three flavors still form Cooper pairs, there are regions of momentum space in which there is no $\langle ds \rangle$ pairing, and other (very narrow) regions in which there is no $\langle us \rangle$ pairing, and these regions are bounded by momenta at which the relevant fermionic quasiparticles are gapless.

The gCFL phase is an electromagnetic conductor: unlike the CFL phase, it contains electrons [3, 4]. The electron chemical potential μ_e increases as M_s^2/μ is increased, rising from zero at the CFL→gCFL transition to values which are comparable to or even larger than its typical values in unpaired quark matter, which has $\mu_e \simeq M_s^2/4\mu$.

C. The gCFL domain

To discuss the range of densities over which gCFL is expected to occur, we shall parametrize the strength of the attractive interaction between quarks by Δ_0 , which we define as the value of the CFL gap parameter at $M_s = 0$ in quark matter with $\mu = 500$ MeV. (We shall quote all numerical results at $\mu = 500$ MeV, corresponding to baryon densities between $8.8 n_0$ and $9.1 n_0$ depending on the value of Δ_0 that we choose, where $n_0 = 0.17 \text{ fm}^{-3}$ is the baryon density in nuclear matter.) Because asymptotic-density calculations are not quanti-

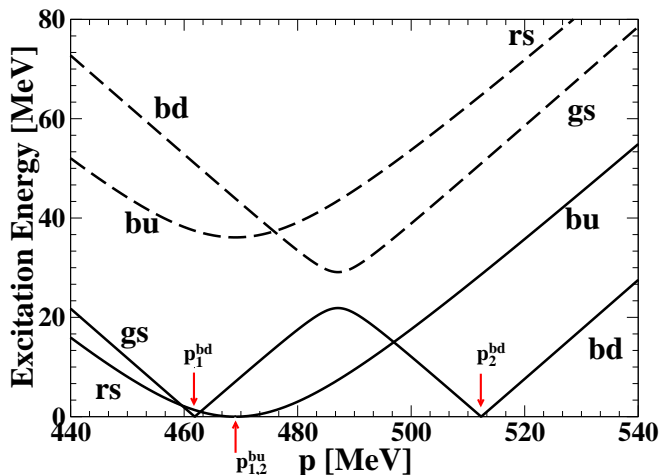


FIG. 1: Dispersion relations for quasiquarks with gs - bd pairing ($\Delta_1 = 3.6$ MeV) and bu - rs pairing ($\Delta_2 = 18.5$ MeV), in the model calculation of Refs. [3, 4, 6] done at $\mu = 500$ MeV, $M_s^2/\mu = 100$ MeV, with $\Delta_0 = 25$ MeV. We find gapless gs - bd modes at $p_1^{bd} = 461$ MeV and $p_2^{bd} = 512$ MeV. One bu - rs mode is gapless with an almost exactly quadratic dispersion relation. Actually it is gapless at two momenta p_1^{bu} and p_2^{bu} , but these are too close together to be resolved until the temperature drops below the eV scale, meaning we can treat them as a single zero at $p_{1,2}^{bu} = 469$ MeV. The five quark quasiparticles not plotted are all fully gapped in the CFL and gCFL phases.

tatively valid at this μ , Δ_0 is not known precisely, with estimates ranging from 10 to 100 MeV [1].

The gCFL phase extends over a range of M_s^2/μ from the continuous CFL→gCFL transition at $M_s^2/\mu = 2\Delta_1 \simeq 2\Delta_0$ up to a first order phase transition where gCFL gives way to some phase with even less pairing. In model calculations, this transition occurs at $M_s^2/\mu \simeq 5\Delta_0$, although this is only quantitatively determined within particular models [3, 4, 5, 6]. To give a sense of the scales involved, for $\Delta_0 = 25$ MeV and $M_s = 250$ MeV, the gCFL window $2\Delta_0 \lesssim M_s^2/\mu \lesssim 5\Delta_0$ corresponds to 320 MeV $\lesssim \mu \lesssim 800$ MeV. At the lower end of this range in μ (upper end in M_s^2/μ) hadronic matter would be more favorable than any form of quark matter. And, the upper end of this range in μ (lower end in M_s^2/μ) corresponds to densities much higher than those achievable in neutron stars. Hence, with these choices of parameters all the quark matter within neutron stars would be in the gCFL phase. For larger Δ_0 or smaller M_s , the gCFL window shifts to lower μ , and neutron stars with a CFL core surrounded by a gCFL layer become possible. In reality, both Δ_0 and M_s are μ -dependent, making these estimates illustrative only.

D. Gapless quasiparticles in the gCFL phase

In the CFL phase, all nine fermionic quasiparticles are gapped. In the gCFL phase, two dispersion relations are

gapless, as shown in Fig. 1. We label the three quark colors as r, g, b , and make the by now conventional choice for which colors pair with which flavors in the CFL phase. In this notation one of the gapless branches describes quasiparticle excitations that are superpositions of bd particles and gs holes. These excitations are gapless at two momenta p_1^{bd} and p_2^{bd} shown in Fig. 1 and given by [4]

$$\frac{1}{2}(\mu_{gs} + \mu_{bd}) \pm \sqrt{\left[\frac{1}{2}(\mu_{gs} - \mu_{bd})\right]^2 - \Delta_1^2}, \quad (1)$$

where μ_{gs} and μ_{bd} are determined by the (nontrivial) requirements of color and electric neutrality. They are defined in Ref. [4], and their values as a function of M_s^2/μ at various Δ_0 can be determined from plots in Refs. [4, 6]. The gapless excitations at p_1^{bd} are predominantly gs , with bd contributing only a small component in the superposition. Those at p_2^{bd} are predominantly bd . In Section IV we shall focus on this dispersion relation in the vicinity of p_1^{bd} , where it takes the form

$$\epsilon_{bd}(p) = v_{bd}|p - p_1^{bd}|, \quad (2)$$

where

$$v_{bd} = \sqrt{1 - \frac{\Delta_1^2}{\left[\frac{1}{2}(\mu_{gs} - \mu_{bd})\right]^2}} \quad (3)$$

is the Fermi velocity of the gapless quasiparticles. The bd states with momenta between p_1^{bd} and p_2^{bd} are filled, whereas the gs states in this momentum range are empty. This means that there is no gs - bd pairing in the ground state wave function in this region of momentum space, although (as the dispersion relations show) there is still pairing among the excitations. The width $p_2^{bd} - p_1^{bd}$ of this “blocking region” wherein pairing is “breached” is zero at the CFL→gCFL phase transition, and grows steadily with increasing M_s^2/μ throughout the gCFL phase. These dispersion relations behave similarly to those describing the gapless modes in the two-flavor gapless 2SC phase [38], and in a metastable three-flavor phase discovered in an early analysis in which the constraints imposed by neutrality were not considered [39].

The physics of the gapless bu - rs dispersion relation is interestingly different. As above these excitations are gapless at two momenta p_1^{bu} and p_2^{bu} given by

$$\frac{1}{2}(\mu_{bu} + \mu_{rs}) \pm \sqrt{\left[\frac{1}{2}(\mu_{bu} - \mu_{rs})\right]^2 - \Delta_2^2}, \quad (4)$$

but in this instance $[\frac{1}{2}(\mu_{bu} - \mu_{rs})]^2 - \Delta_2^2$ is *very* small, making the dispersion relation in Fig. 1 look quadratic with a single zero at $p_{1,2}^{bu} = \frac{1}{2}(\mu_{bu} + \mu_{rs})$. For the parameters of Fig. 1, $p_2^{bu} - p_1^{bu} = 0.026$ MeV and the height of the dispersion relation half way between these very nearby gapless points is only about 5 eV. Since this is much smaller than the temperatures that will be of interest to us, we can safely treat the dispersion relation as quadratic, with a dispersion relation in the vicinity of

its gapless point given approximately by

$$\epsilon_{bu}(p) = \frac{(p - p_{1,2}^{bu})^2}{2\Delta_2}, \quad (5)$$

with the velocity v_{bu} , defined analogously to v_{bd} of (3), vanishing at the gapless point. The gap parameter Δ_2 and the chemical potentials that determine $p_{1,2}^{bu}$ are plotted as functions of M_s^2/μ at several values of Δ_0 in Refs. [4, 6].

This near-quadratic dispersion relation is not a result of fine tuning. It occurs at all μ in the gCFL phase, and arises from the fact that bulk matter must be electrically and color neutral [3, 4]. In both the CFL and gCFL phase, there is an unbroken gauge symmetry, denoted $U(1)_{\tilde{Q}}$, generated by a linear combination of the generators of electromagnetic and color symmetry [2]. Among the neutrality constraints, it is the imposition of \tilde{Q} -neutrality that has the implication of interest. The quarks in the gCFL phase are almost \tilde{Q} -neutral by themselves, but not quite: their small excess positive \tilde{Q} charge is cancelled by a small admixture of electrons, which have $\tilde{Q} = -1$. The excess of unpaired bd -quarks, occurring in a broad band of momenta $p_1^{bd} < p < p_2^{bd}$, does not contribute to the \tilde{Q} imbalance because these quarks have $\tilde{Q} = 0$. It is the unpaired bu -quarks with $p_1^{bu} < p < p_2^{bu}$ that matter, because they have $\tilde{Q} = +1$. They contribute a positive \tilde{Q} -charge density of order $\mu^2(p_2^{bu} - p_1^{bu})$, balanced by the electron number density, of order μ_e^3 . Since $\mu_e \ll \mu$ throughout the gCFL phase, $p_2^{bu} - p_1^{bu}$ is forced (by the dynamics of the gauge fields that maintain neutrality) to remain extremely small, parametrically of order μ_e^3/μ^2 , throughout the gCFL phase.

As described above, the dispersion relations for the gs - bd quasiparticles are linear about their gapless momenta p_1^{bd} and p_2^{bd} , as in Eq. (2), at generic values of M_s^2/μ in the gCFL phase. However, this dispersion relation is fine-tuned to be quadratic precisely at the CFL→gCFL transition, where $p_1^{bd} = p_2^{bd}$ and the Fermi velocity $v_{bd} = 0$. For values of M_s^2/μ that are in the gCFL regime but are close to the CFL→gCFL transition, therefore, the simplified linear expression in Eq. (2) cannot be used. Indeed, if we are interested in those excitations with energies of order T or less, the linear expression in Eq. (2) is a good approximation as long as $v_{bd} \gtrsim \sqrt{2T/\Delta_1}$. And, close enough to the transition that $v_{bd} \ll \sqrt{2T/\Delta_1}$ the gs - bd

dispersion relation can be approximated as quadratic, as is appropriate for the bu - rs dispersion relation throughout the gCFL phase.

The gapless excitations of the gCFL phase whose dispersion relations we have described determine the specific heat and neutrino emissivity of this phase of matter. In the next two sections, we calculate these quantities in turn.

III. SPECIFIC HEAT OF GAPLESS CFL QUARK MATTER

The specific heat of any phase of matter is essentially a count of the number of possible excitations with excitation energies of order T or smaller. Precisely, the contribution of quasiparticle excitations with dispersion relation $\epsilon(p)$ to the specific heat (heat capacity per unit volume) at temperature T is given by

$$\begin{aligned} c_V &= 2 \int \frac{d^3p}{(2\pi)^3} \epsilon(p) \frac{d}{dT} \left(\frac{1}{e^{\epsilon(p)/T} + 1} \right) \\ &= \frac{2}{T^2} \int \frac{d^3p}{(2\pi)^3} \frac{\epsilon(p)^2}{(e^{\epsilon(p)/T} + 1)(e^{-\epsilon(p)/T} + 1)} \end{aligned} \quad (6)$$

where the prefactor 2 assumes that the quasiparticle is doubly degenerate by virtue of its spin. Clearly, only those excitations with $\epsilon \lesssim T$ are important. For the gapless quasiparticle with quadratic dispersion relation, ϵ is near zero for p near $p_{1,2}^{bu}$ and in this regime the dispersion relation can be approximated as in (5). Approximating the dispersion relation in this way will give us the specific heat in the small T limit, and so although it is straightforward to obtain an “exact” result upon assuming (5), we simply quote the leading result in the small T limit:

$$\begin{aligned} c_V &= \frac{3(\sqrt{2} - 1)\zeta\left(\frac{3}{2}\right)}{4\pi^{3/2}} (p_{1,2}^{bu})^2 \Delta_2^{1/2} T^{1/2} \\ &\simeq 0.146 (p_{1,2}^{bu})^2 \Delta_2^{1/2} T^{1/2}. \end{aligned} \quad (7)$$

As expected, this is proportional to the number of excitations with energy less than T , given a quadratic dispersion relation (5). For quasiparticles with conventional linear dispersion relations, namely $\epsilon(p) = v|p - p_F|$ for some p_F and v , the expression (6) yields the familiar $c_V = \frac{1}{3}p_F^2 T/v$. Hence, the specific heat of the gCFL phase is given by

$$c_V = \frac{k_B}{(\hbar c)^3} \left[0.146 (p_{1,2}^{bu} c)^2 \Delta_2^{1/2} (k_B T)^{1/2} + \frac{c}{3v_{bd}} (p_1^{bd} c)^2 k_B T + \frac{c}{3v_{bd}} (p_2^{bd} c)^2 k_B T + \frac{1}{3} \mu_e^2 k_B T \right], \quad (8)$$

where we have restored factors of \hbar , c and Boltzmann’s constant k_B and where the last term comes from the electrons and is negligible because all the quark Fermi mo-

menta are of order μ , and $\mu_e \ll \mu$. As long as $T \ll \Delta_2$, the contribution from the quasiparticle with quadratic dispersion relation dominates. We shall describe reason-

able values of Δ_2 and T in subsequent sections; it suffices here to say that Δ_2/T is of order hundreds or thousands.

Note that close enough to the CFL→gCFL transition that $v_{bd} \lesssim \sqrt{2T/\Delta_1}$, the gs - bd dispersion relation cannot be treated as linear, and the expression (8) is modified. Indeed, if $v_{bd} \ll \sqrt{2T/\Delta_1}$ the gs - bd dispersion relation can be treated as quadratic, making their contribution to the specific heat comparable to that of the bu - rs quasiparticles.

The gCFL phase also has light bosonic excitations, for example that associated with superfluidity, but their contribution to the specific heat is of order T^3 and so can be neglected. The specific heat may be enhanced by logarithmic corrections analogous to those in unpaired quark matter [40], but we leave their analysis to future work.

IV. NEUTRINO EMISSIVITY OF GAPLESS CFL QUARK MATTER

The presence of gapless quark quasiparticles in the gCFL phase raises the possibility of neutrino emission by direct Urca processes. Because the gapless modes are superpositions of gs and bd quarks, and bu and rs quarks, and because weak interactions cannot change the color of a quark, the direct Urca processes that we must consider are

$$bd \rightarrow bu + e^- + \bar{\nu} \quad (9)$$

and

$$bu + e^- \rightarrow bd + \nu. \quad (10)$$

Momentum conservation in these reactions requires that the momenta of the two quarks and the electron form a triangle [28]. (The argument is that these three fermions must all have energies of order T and hence must all be close to the momenta at which their dispersion relations are gapless. The neutrinos escape from the star, and hence have zero Fermi momentum. By energy conservation, the escaping neutrino therefore has energy, and hence momentum, of order T . This is negligible compared with the momenta of the other fermions.) Momenta of the two quarks and the electron satisfying the triangle constraint can only be found if $|p^{bu} - p^{bd}| \leq \mu_e$, where p^{bu} and p^{bd} are the magnitudes of the momenta at which the bu and bd quarks are gapless. The only momentum at which gapless quasiparticles with a bu component are found is $p_{1,2}^{bu}$. Gapless bd quarks occur at two momenta. For the parameters in Fig. 1, the electron Fermi momentum is $\mu_e = 25.9$ MeV, meaning that the triangle constraint can be satisfied if we choose bd quarks with momenta near p_1^{bd} , but cannot be satisfied for those near p_2^{bd} . Indeed, we find that direct Urca processes involving the quasiparticles at p_2^{bd} are forbidden throughout the gCFL regime of M_s^2/μ , whereas those involving quasiparticles at p_1^{bd} are allowed throughout all of the gCFL regime, with the available phase space vanishing at the

CFL→gCFL transition and opening up with increasing M_s^2/μ .

The calculation of the neutrino emissivity due to direct Urca processes in unpaired quark matter was first done by Iwamoto in Ref. [28], and we shall follow his analysis, leaving the calculation of any logarithmic enhancement analogous to that in unpaired quark matter [41] to future work. There are two essential differences between Iwamoto's calculation for unpaired quark matter and ours for the gCFL phase. First, although the quasiparticles near p_1^{bd} have a conventional linear dispersion relation $\epsilon_{bd}(p)$ given in (2), as in unpaired quark matter, the quasiparticles near $p_{1,2}^{bu}$ have a quadratic dispersion relation $\epsilon_{bu}(p)$ given in (5). Analogous to its effect on the specific heat, this unusual dispersion relation increases the available phase space for the direct Urca reactions by a factor of order $\sqrt{\Delta_2/T}$ relative to that in the standard calculation, resulting in a neutrino emissivity $\epsilon_\nu \sim T^{5.5}$ rather than $\sim T^6$. Second, the quasiparticles near p_1^{bd} and $p_{1,2}^{bu}$ with dispersion relations ϵ_{bd} and ϵ_{bu} are *not* purely bd and bu quarks. They are superpositions of bd and gs quarks, and bu and rs quarks, respectively. Only the bd and bu components of the quasiparticles participate, meaning that the neutrino emissivity is proportional to the probabilities that each quasiparticle is blue. These probabilities are the squares of the Bogoliubov coefficients B_{bu} and B_{bd} , specified as follows [2]. B_{bu} is given by

$$B_{bu}(p)^2 = \frac{1}{2} \left(1 + \frac{p - p_{1,2}^{bu}}{\sqrt{(p - p_{1,2}^{bu})^2 + \Delta_2^2}} \right) \quad (11)$$

where $p_{1,2}^{bu} = \frac{1}{2}(\mu_{bu} + \mu_{rs})$ and where Δ_2 is the gap parameter for the pairing between bu and rs quarks. To simplify the calculation we Taylor expand the coefficient around $p_{1,2}^{bu}$ and get

$$B_{bu}(p)^2 = \frac{1}{2} \left(1 + \frac{p - p_{1,2}^{bu}}{\Delta_2} \right). \quad (12)$$

The bd Bogoliubov coefficient is given by

$$B_{bd}(p)^2 = \frac{1}{2} \left(1 + \frac{p - \bar{\mu}}{\sqrt{(p - \bar{\mu})^2 + \Delta_1^2}} \right) \quad (13)$$

where $\bar{\mu} = \frac{1}{2}(\mu_{bd} + \mu_{gs})$ and where Δ_1 is the gap parameter for the pairing between bd and gs quarks. Because the dispersion relation is linear, the quarks that contribute to the emissivity lie in a band about p_1^{bd} whose width is only of order T , and we shall replace $B_{bd}(p)$ by $B_{bd}(p_1^{bd})$. This coefficient can be quite small. For example, with parameters as in Fig. 1, meaning in particular $M_s^2/\mu = 100$ MeV, the probability that the gapless quasiparticles at p_1^{bd} are in fact bd is only $B_{bd}(p_1^{bd})^2 = 0.00479$.

We now present the calculation of ϵ_ν , following Ref. [28]. The transition rate for the process (9) is

$$W = \frac{V(2\pi)^4 \delta^{(4)}(p_{bd} - p_\nu - p_{bu} - p_e)}{\prod_{i=1}^4 2E_i V} |M|^2 \quad (14)$$

where the index i runs over the four species that participate in the interaction. V is the normalization volume, which will drop out by the end of the calculation, and the squared amplitude $|M|^2$ is given by

$$|M|^2 = 64G_F^2 \cos^2 \theta_c (p_{bd} \cdot p_\nu)(p_{bu} \cdot p_e), \quad (15)$$

where we have averaged over the spin of the initial down quark and summed over the spin of the final up quark.

Here, G_F is the Fermi constant and θ_c is the Cabibbo angle.

The neutrino emissivity is the rate of energy loss per unit volume due to neutrino emission. It is obtained by multiplying the transition rate by the neutrino energy and integrating over the available phase space, weighted by the Bogoliubov coefficients. The expression can be written as

$$\varepsilon_\nu = \frac{2}{V} \left[\prod_{i=1}^4 V \int \frac{d^3 p_i}{(2\pi)^3} \right] E_\nu W n(p_{bd})(1 - n(p_{bu}))(1 - n(p_e)) B_{bu}(p_{bu})^2 B_{bd}(p_1^{bd})^2. \quad (16)$$

Here, the Fermi distribution functions $n(p_{bd})(1 - n(p_{bu}))(1 - n(p_e))$ state that in order for the process to occur we have to have an occupied down state and unoccupied up and electron states. In thermal equilibrium (which is maintained by strong and electromagnetic processes occurring on timescales much faster than neutrino emission via weak interactions) the distribution functions are given by

$$n(p_i) = \frac{1}{1 + \exp x_i} \quad (17)$$

where

$$x_e = \frac{p_e - \mu_e}{T}, \quad (18)$$

where

$$x_{bd} = \pm \frac{\epsilon_{bd}(p_{bd})}{T}, \quad (19)$$

with the \pm serving in effect to undo the absolute value in (2), and where

$$x_{bu} = \pm \frac{\epsilon_{bu}(p_{bu})}{T} \quad (20)$$

with the \pm chosen positive for $p_{bu} > p_{1,2}^{bu}$ and negative for $p_{bu} < p_{1,2}^{bu}$. In defining x_{bd} we have used (2), meaning that this derivation is valid at generic values of M_s^2/μ in the gCFL regime where $v_{bd} \gtrsim \sqrt{2T/\Delta_1}$, but not close to the CFL→gCFL transition, where both the bd and bu branches should be treated as quadratic. We shall discuss this further below. For later use, we also define

$$x_\nu = \frac{p_\nu}{T}. \quad (21)$$

It is possible to set the calculation up directly in terms of the positive quasiparticle excitation energies, but introducing the \pm as we have done allows us to follow Iwamoto's calculation more closely.

We combine Eqs. (14), (15), (16), (17) and multiply by a factor of 2 in order to include the emissivity due to the second process (10), whose contribution proves to be the same as that above. We write the integration element $d^3 p_i = p_i^2 dp_i d\Omega_i$, where $d\Omega_i$ is the infinitesimal solid angle. The complete expression for the emissivity then takes the form [28]

$$\varepsilon_\nu = \frac{G_F^2}{16\pi^8} \cos^2 \theta_c (1 - \cos \theta_{ue}) \mathcal{A} \mathcal{B}. \quad (22)$$

Here, \mathcal{A} is an angular integral defined as

$$\mathcal{A} = \left(\prod_{i=1}^4 \int d\Omega_i \right) \delta(\mathbf{p}_{bd} - \mathbf{p}_{bu} - \mathbf{p}_e), \quad (23)$$

where we have eliminated certain terms that vanish identically upon angular integration. \mathcal{A} is identical to that in Ref. [28] and upon evaluation yields

$$\mathcal{A} = \frac{32\pi^3}{p_1^{bd} p_{1,2}^{bu} \mu_e}, \quad (24)$$

where we have taken $|\mathbf{p}_{bd}| = p_1^{bd}$, $|\mathbf{p}_{bu}| = p_{1,2}^{bu}$, $|\mathbf{p}_e| = \mu_e$, knowing that these are the values at which the \mathcal{B} integral is dominated. The integral \mathcal{B} is defined as

$$\mathcal{B} = \int_0^\infty p_{bd}^2 dp_{bd} \int_0^\infty p_{bu}^2 dp_{bu} \int_0^\infty p_e^2 dp_e \int_0^\infty p_\nu^3 dp_\nu n(p_{bd})(1-n(p_{bu}))(1-n(p_e)) \times \frac{1}{T} \delta(x_{bd} - x_\nu - x_{bu} - x_e) B_{bu}(p_{bu})^2 B_{bd}(p_1^{bd})^2. \quad (25)$$

Finally, the angle θ_{ue} in (22) is the angle between the momentum of the bu -quark and that of the electron, when the two quark momenta and the electron momentum are arranged in a momentum conserving triangle. A little trigonometry shows that $\theta_{ue} = \theta_{de} + \theta_{du}$ where

$$\cos \theta_{de} = \frac{(p_1^{bd})^2 + \mu_e^2 - (p_{1,2}^{bu})^2}{2p_1^{bd}\mu_e} \quad (26)$$

and

$$\cos \theta_{du} = \frac{(p_1^{bd})^2 - \mu_e^2 + (p_{1,2}^{bu})^2}{2p_1^{bd}p_{1,2}^{bu}}. \quad (27)$$

Now, all that remains is the evaluation of \mathcal{B} .

The integral \mathcal{B} is dominated by p_{bd} near p_1^{bd} , by p_{bu} near $p_{1,2}^{bu}$, and by p_e near μ_e so we can pull the factor $p_{bd}^2 p_{bu}^2 p_e^2$ out of the integrand and replace it by $(p_1^{bd})^2 (p_{1,2}^{bu})^2 \mu_e^2$. Next, we change variables of integration from the p 's to the x 's and obtain

$$\mathcal{B} = (p_1^{bd})^2 (p_{1,2}^{bu})^2 \mu_e^2 T^6 \frac{B_{bd}(p_1^{bd})^2}{2} \int_{-\infty}^\infty \frac{dx_{bd}}{v_{bd}} \int_{-\infty}^\infty dx_e \int_0^\infty dx_\nu x_\nu^3 \int_{-\infty}^\infty dx_{bu} \frac{\sqrt{\Delta_2}}{\sqrt{2T}|x_{bu}|} \frac{1}{e^{x_{bd}} + 1} \frac{1}{e^{x_{bu}} + 1} \frac{1}{e^{x_e} + 1} \times \delta(x_{bd} + x_{bu} + x_e - x_\nu) \quad (28)$$

where, as in the calculation of the specific heat, the enhanced density of states $dp_{bu}/dx_{bu} = (\Delta_2 T/2 |x_{bu}|)^{1/2}$ for the quasiparticle with the quadratic dispersion relation is crucial. In (28) we have made the approximation $B_{bu}(p_{1,2}^{bu})^2 \simeq \frac{1}{2}$, since the other term in (12) leads to a contribution proportional to T^6 and we are keeping only the leading contribution, proportional to $T^{5.5}$. We now rewrite (28) as

$$\mathcal{B} = \frac{1}{2\sqrt{2}} (p_1^{bd})^2 (p_{1,2}^{bu})^2 \mu_e^2 \frac{T^{5.5} \sqrt{\Delta_2} B_{bd}(p_1^{bd})^2}{v_{bd}} \int_{-\infty}^\infty dx_{bd} \int_{-\infty}^\infty dx_e \int_0^\infty dx_\nu x_\nu^3 \int_{-\infty}^\infty dx_{bu} \frac{1}{\sqrt{|x_{bu}|}} \frac{1}{e^{x_{bd}} + 1} \frac{1}{e^{x_{bu}} + 1} \frac{1}{e^{x_e} + 1} \times \delta(x_{bd} + x_{bu} + x_e - x_\nu), \quad (29)$$

use the delta function to perform one of the integrations, and then perform the remaining dimensionless triple integral numerically. The result is

$$\mathcal{B} = 31.18 (p_1^{bd})^2 (p_{1,2}^{bu})^2 \mu_e^2 \frac{T^{5.5} \sqrt{\Delta_2} B_{bd}(p_1^{bd})^2}{v_{bd}}. \quad (30)$$

Combining this with the result (24) for \mathcal{A} and substituting into (22) we obtain the final result for the neutrino emissivity of the gCFL phase

$$\varepsilon_\nu = \frac{62.36}{\pi^5} \frac{G_F^2 \cos^2 \theta_c}{\hbar^{10} c^7} (1 - \cos \theta_{ue}) p_1^{bd} p_{1,2}^{bu} \mu_e \frac{(k_B T)^{5.5} \sqrt{\Delta_2} B_{bd}(p_1^{bd})^2}{v_{bd}}, \quad (31)$$

where we have restored the factors of \hbar , c and k_B . This result is valid as long as $v_{bd} \gtrsim \sqrt{2T/\Delta_1}$, meaning that the gs - bd dispersion relation can be treated as linear with slope v_{bd} . At any nonzero temperature, there is a region just on the gCFL side of the CFL \rightarrow gCFL transition where this approximation breaks down. Indeed, in the region so close to the transition that $v_{bd} \ll \sqrt{2T/\Delta_1}$, the gs - bd and bu - rs dispersion relations can both be treated as quadratic, and an analysis similar to that we have presented above yields

$$\varepsilon_\nu = \frac{42.70}{\pi^5} \frac{G_F^2 \cos^2 \theta_c}{\hbar^{10} c^7} (1 - \cos \theta_{ue}) p_1^{bd} p_{1,2}^{bu} \mu_e (k_B T)^5 \sqrt{\Delta_2 \Delta_1} B_{bd}(p_1^{bd})^2. \quad (32)$$

We shall see below that for temperatures of interest in neutron star physics, this expression is valid only in a

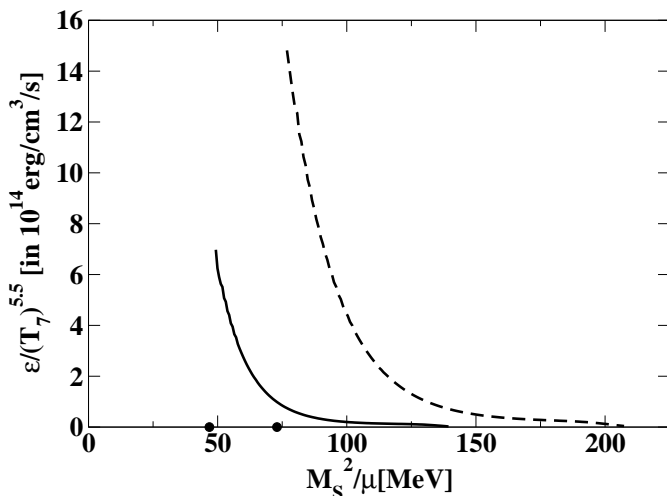


FIG. 2: Neutrino emissivity ε_ν of gCFL quark matter from (31) divided by $(T/10^7\text{K})^{5.5}$, plotted versus M_s^2/μ . The two curves are drawn for two different values of the strength of the interaction between quarks, corresponding to CFL gap parameters $\Delta_0 = 25$ (solid curve) and $\Delta_0 = 40$ MeV (dashed). The location of the CFL \rightarrow gCFL transitions for $\Delta_0 = 25$ and 40 MeV are indicated by dots on the horizontal axis, at $M_s^2/\mu = 46.8$ and 73.0 MeV respectively. To the left of these dots, ε_ν is negligible in the CFL phase. As discussed in the text we begin the curves a small interval to the right of the transition, at the M_s^2/μ where $v_{bd} = 0.15$. (The $\Delta_0 = 25$ MeV and $\Delta_0 = 40$ MeV curves begin 2.5 MeV and 3.9 MeV to the right of their respective transitions.) The baryon chemical potential is $\mu = 500$ MeV, corresponding to a density about nine times that of ordinary nuclear matter. The effect of changing μ while keeping M_s^2/μ and Δ_0 fixed can be approximated by scaling ε_ν with μ^2 .

very narrow window of parameter space. It is (31) that is relevant to neutron star phenomenology.

The gCFL emissivity (31) can be compared to the neutrino emissivity of noninteracting quark matter [28]

$$\begin{aligned} \varepsilon_\nu^{\text{unpaired}} &= \frac{457\pi}{1680} \frac{G_F^2 \cos^2 \theta_c}{\hbar^{10} c^4} M_s^2 p_F (k_B T)^6 \\ &= (3.6 \times 10^{14} \text{ erg cm}^{-3} \text{ s}^{-1}) \times \\ &\quad \left(\frac{M_s^2/\mu}{100 \text{ MeV}} \right) \left(\frac{\mu}{500 \text{ MeV}} \right)^2 \left(\frac{T}{10^7 \text{ K}} \right)^6 \end{aligned} \quad (33)$$

where $p_F \simeq \mu$ is the up quark Fermi momentum and where μ_e has been replaced by $M_s^2/4\mu$, appropriate for neutral unpaired quark matter. The gCFL emissivity (31) is enhanced by a factor of $\sqrt{\Delta_2/T}$ relative to that of noninteracting quark matter, but the full comparison between the two rates is more involved.

We have obtained our result (31) in a form which makes the dependence of ε_ν on T manifest, but which obscures the dependence on M_s and μ because Δ_2 , $B_{bd}(p_1^{bd})$, μ_e , v_{bd} , p_1^{bd} and $p_{1,2}^{bu}$ all change with M_s and μ . The most important μ dependence is straightforward: $p_1^{bd} \sim p_{1,2}^{bu} \sim \mu$ and hence $\varepsilon_\nu \sim \mu^2$. The remaining dependence on M_s and μ is dominated by the dependence on

M_s^2/μ , which is nontrivial because Δ_2 , $B_{bd}(p_1^{bd})$, μ_e and v_{bd} and $p_2^{bd} - p_1^{bd}$ all depend nontrivially on M_s^2/μ . The result also depends on Δ_0 , through this same set of quantities. The reader who wishes to obtain numerical values of ε_ν would need numerical values for the gap parameters and chemical potentials in the gCFL phase given in plots in Refs. [4, 6], which are used in the specification of many of the quantities occurring in (31). Given all these implicit dependences, we provide Fig. 2 for the convenience of the reader who wishes to use our result (31) for the gCFL neutrino emissivity, for example in order to calculate its effects on neutron star cooling.

The most important dependences of ε_ν are straightforward: $\varepsilon_\nu \sim T^{5.5}$ and $\varepsilon_\nu \sim \mu^2$. All the remaining dependences are best described as dependence on M_s^2/μ and Δ_0 , and hence are described by Figure 2 which shows $\varepsilon_\nu/T^{5.5}$ as a function of M_s^2/μ for two values of Δ_0 . For each Δ_0 , we see nonzero neutrino emissivity in the corresponding gCFL regime, with ε_ν negligible at lower M_s^2/μ in the CFL phase. We do not plot ε_ν at values of M_s^2/μ that are larger than the gCFL regime, because it is not known what phase of quark matter would be favored there, with what T -dependence for its ε_ν . (Crystalline color superconducting quark matter [17] is a leading candidate for the third-densest phase on the QCD phase diagram, and its neutrino emissivity has not been calculated.) Also, at these low densities quark matter may well have already been superseded by nuclear matter. Note that a reasonable estimate of the range of M_s^2/μ of interest to describe possible quark matter in neutron stars is $50 \text{ MeV} < M_s^2/\mu < 250 \text{ MeV}$, corresponding roughly to $350 \text{ MeV} < \mu < 500 \text{ MeV}$ and $150 \text{ MeV} < M_s < 300 \text{ MeV}$. If Δ_0 is large, say $\Delta_0 = 100$ MeV, the curve on Fig. 2 shifts far to the right, and any quark matter that occurs is likely CFL, with negligible ε_ν . We see from the figure that for $\Delta_0 = 25$ MeV, the highest density quark matter that can be reached is likely in the gCFL phase. For intermediate values of Δ_0 , it is possible to obtain a CFL core surrounded by a gCFL layer.

The shape of the curves in Fig. 2 arises from the combination of many effects. As M_s^2/μ increases through the gCFL regime, μ_e rises monotonically and $(1 - \cos \theta_{ue})$ initially rises rapidly as phase space for neutrino emission opens up, and then varies little. These effects are overwhelmed by the fact that as M_s^2/μ increases through the gCFL regime, Δ_2 , $1/v_{bd}$, and the Bogoliubov coefficient $B_{bd}(p_1^{bd})$ all decrease monotonically.

Close to the CFL \rightarrow gCFL transition, the most important contribution to the steep decrease of ε_ν with increasing M_s^2/μ seen in Fig. 2 is the factor $1/v_{bd}$ occurring in (31), since after all $v_{bd} = 0$ at the transition. However, one must recall that the expression (31) plotted in Fig. 2 is only valid for $v_{bd} \gtrsim \sqrt{2T/\Delta_1}$. Indeed, for any nonzero T there is a region close to the transition where $v_{bd} \ll \sqrt{2T/\Delta_1}$ and the emissivity is given by (32) with $\varepsilon_\nu \sim T^5$, not by (31) with $\varepsilon_\nu \sim T^{5.5}$ as plotted in Fig. 2. In Fig. 2, we have begun the gCFL curves at the value of

M_s^2/μ at which $v_{bd} = 0.15$, meaning that the curves can be trusted as long as $T \lesssim \Delta_1/100 \simeq \Delta_0/100$. (Note that $\Delta_1 \simeq \Delta_0$ near the CFL \rightarrow gCFL transition.) For typical neutron star temperatures of order keV, $\varepsilon_\nu \sim T^{5.5}$ as given by (31) (and the curves of Fig. 2 are therefore valid) even closer to the transition than where we stopped the curves in the Fig 2. The curves can safely be used in neutron star cooling calculations, as we shall do in Section V.

Further to the right in Fig. 2, well away from the transition, v_{bd} approaches 1 and the factor $1/v_{bd}$ ceases to control the shape of the curves. In this regime, the most important contribution to the decline in ε_ν is the rapidly falling Bogoliubov coefficient: as M_s^2/μ increases p_1^{bd} and p_2^{bd} in Fig. 1 separate and the bd -component of the gapless quasiparticle at p_1^{bd} , namely $B_{bd}(p_1^{bd})$, drops faster than μ_e rises.

In Section V we shall sketch the implications of our results for the specific heat and neutrino emissivity of gCFL quark matter for neutron star cooling. The most important dependence of ε_ν in this context is its T -dependence. In all plots in Section V, we show two curves, both with $M_s^2/\mu = 100$ MeV, one with $\Delta_0 = 25$ MeV and one with $\Delta_0 = 40$ MeV. We choose these values because we see from Fig. 2 that they correspond to a small, but reasonable, and a larger, but still reasonable, value of $\varepsilon_\nu/T^{5.5}$. Were we to choose values of parameters that happened to land very close to the CFL \rightarrow gCFL transition, all the conclusions that we draw in the next section would become stronger.

V. IMPLICATIONS FOR THE COOLING OF NEUTRON STARS

The central results of this paper are the specific heat and neutrino emissivity, calculated in Sections III and IV. We shall not attempt a state-of-the-art neutron star cooling calculation here, preferring instead to provide a calculation that is better thought of as illustrative, not quantitative. The effect that we wish to highlight is both large and qualitative, arising from the T -dependence of c_V and ε_ν , and we expect that even our crude treatment will persuade the reader of its significance.

We analyze the cooling of a “toy star” consisting of a volume of “nuclear matter” at a constant density $1.5n_0$ and a volume of denser quark matter with a constant density specified by $\mu = 500$ MeV. As nuclear matter we take an electrically neutral gas of noninteracting neutrons, protons and electrons in weak equilibrium. We investigate three different possibilities for the quark matter, all electrically and color neutral and in weak equilibrium, and all with $\mu = 500$ MeV and $M_s^2/\mu = 100$ MeV. We consider two possibilities for quark matter in the gCFL phase, with $\Delta_0 = 40$ MeV and $\Delta_0 = 25$ MeV. And, we consider noninteracting quark matter. These three options have densities of 9.1, 8.9 and 8.8 times normal nuclear matter density n_0 , respectively. By treat-

ing the quark matter core as having a constant density, our calculation neglects the possibility of a thin spherical gCFL-CFL interface region, in which there would be an enhancement in both the specific heat (by a factor of two, see end of Sect. III) and the neutrino emissivity (see Eq. (32)) relative to the gCFL expressions (8) and (31) that we shall use. Such a shell would be very thin because these enhancements occur only within a very narrow window in M_s^2/μ , but a quantitative investigation of how small its effects are is not possible in our “toy star calculation”. We choose the quark matter and nuclear matter volumes V_{qm} and V_{nm} such that the total mass of the star is 1.4 solar masses. If we set the quark matter volume to zero, this corresponds to choosing a nuclear matter “star” that is a sphere with radius $R = 12$ km. If we include a dense quark matter core with radius R_{core} while keeping the total mass fixed, the star shrinks as we increase R_{core} . With $R_{\text{core}} = 5$ km the stellar radius is $R = 10$ km. A gCFL core with radius 5 km has the same volume as a gCFL layer extending from $r = 4.5$ km to $r = 6$ km. Since such a layer would surround a CFL quark matter core, and since CFL matter plays no role in neutron star cooling, the estimates that we quote for $R_{\text{core}} = 5$ km can equally well be taken as a guide to this scenario. Our final toy-model assumption is that our “star” is a black body. The work that needs to be done to turn our illustrative “toy star calculation” into a quantitative calculation of neutron star cooling includes the investigation of realistic density profiles, realistic nuclear matter, and realistic atmospheres. We defer this, as our calculation suffices to make our qualitative point.

Our “star” loses heat by neutrino emission from its entire volume and by black body emission of photons from its surface. The heat loss due to neutrino emission is

$$L_\nu = V_{nm}\varepsilon_\nu^{nm} + V_{qm}\varepsilon_\nu^{qm}. \quad (34)$$

The quark matter neutrino emissivity ε_ν^{qm} is given either by (31) or (33), depending on whether we are considering a gCFL core or an unpaired quark matter core. The nuclear matter emits neutrinos via modified Urca processes like $n + X \rightarrow p + X + e + \bar{\nu}$, with X either a neutron or a proton that serves to carry away some recoil momentum, in order that momentum and energy can both be conserved in the process. The resulting emissivity is [21, 26]

$$\varepsilon_\nu^{nm} = (1.2 \times 10^4 \text{ erg cm}^{-3}\text{s}^{-1}) \left(\frac{n}{n_0}\right)^{2/3} \left(\frac{T}{10^7 \text{ K}}\right)^8. \quad (35)$$

In evaluating the nuclear matter and quark matter emissivities, we shall assume that the entire interior of the star is at a common temperature T . Both nuclear matter and quark matter are good conductors of heat, and neutron stars older than a few years are well approximated as isothermal.

Because $\varepsilon_\nu \sim T^{5.5}$ in the gCFL phase, L_ν will be dominated by neutrino emission from the gCFL matter, unless the gCFL volume is very small. We include cooling

curves for cores made of “unpaired quark matter” even though this is not expected to be present on the phase diagram of QCD at neutron star temperatures because it serves as a representative example of the large class of phases of dense matter in which $\varepsilon_\nu \sim T^6$ and $c_V \sim T$. This class includes all quark and nuclear phases that cool by direct Urca processes, except for gCFL.

The surface of real neutron stars is colder than their interiors, with the temperature gradients occurring only in the outer envelope of the star within of order 100 meters of the surface. The heat transport within this envelope has been analyzed [42], and the result is well approximated by a phenomenological relationship between the interior temperature T and the surface temperature T_{surface} given by [23, 42]

$$T_{\text{surface}} = (0.87 \times 10^6 \text{ K}) \left(\frac{g_s}{10^{14} \text{ cm/s}^2} \right)^{1/4} \left(\frac{T}{10^8 \text{ K}} \right)^{0.55}, \quad (36)$$

where $g_s \equiv G_N M/R^2$ is the surface gravity. This means that the rate of heat loss from the surface of the star, which for a black body is

$$L_\gamma = 4\pi R^2 \sigma T_{\text{surface}}^4 \quad (37)$$

with σ the Stefan-Boltzmann constant, is given by

$$L_\gamma = 4\pi R^2 \sigma (0.87 \times 10^6 \text{ K})^4 \left(\frac{g_s}{10^{14} \text{ cm/s}^2} \right) \left(\frac{T}{10^8 \text{ K}} \right)^{2.2}. \quad (38)$$

We shall use this expression for L_γ , even though we are not treating other aspects of the problem realistically, because the fact that $L_\gamma \sim T^{2.2}$ will play an important qualitative role.

The cooling of our “star” is described by the differential equation

$$\frac{dT}{dt} = -\frac{L_\nu + L_\gamma}{V_{nm}c_V^{nm} + V_{qm}c_V^{qm}} = -\frac{V_{nm}\varepsilon_\nu^{nm} + V_{qm}\varepsilon_\nu^{qm} + L_\gamma}{V_{nm}c_V^{nm} + V_{qm}c_V^{qm}} \quad (39)$$

which equates the heat lost ($\sim Ldt$) to the change in the heat energy of the star ($\sim -Vc_V dT$). We have all the ingredients needed to evaluate the right hand side of this equation in place, with the exception of the specific heat of nuclear matter and of unpaired quark matter. For a gas of several species of noninteracting fermions, the specific heat is given by

$$c_V = \frac{k_B^2 T}{3\hbar^3 c} \sum_i p_F^i \sqrt{m_i^2 c^2 + (p_F^i)^2}, \quad (40)$$

where the sum runs over all the species. In the case of noninteracting nuclear matter, the sum runs over $i = n, p, e$ and the Fermi momenta for neutral matter in weak equilibrium are given by [21]

$$\begin{aligned} p_F^n &= (340 \text{ MeV}) \left(\frac{n}{n_0} \right)^{1/3} \\ p_F^p &= p_F^e = (60 \text{ MeV}) \left(\frac{n}{n_0} \right)^{2/3}. \end{aligned} \quad (41)$$

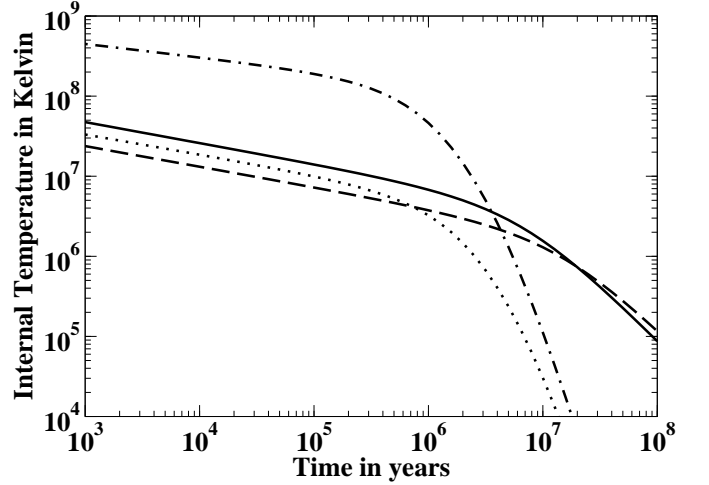


FIG. 3: Solutions to the cooling equation (39) for 1.4 solar mass “toy stars” (described in the text) of four different compositions. The curves show internal temperature as a function of time. The dot-dashed curve is for a star with radius $R = 12$ km made entirely of nuclear matter with a density $1.5n_0$, with no quark matter core. The other three curves describe stars with radii $R = 10$ km that have quark matter cores with radii $R_{\text{core}} = 5$ km. For all three curves, the quark matter has $\mu = 500$ MeV and $M_s^2/\mu = 100$ MeV, with densities $\simeq 9n_0$. For the dotted curve, the quark matter is noninteracting. For the solid (dashed) curve, it is in the gCFL phase with $\Delta_0 = 25$ MeV ($\Delta_0 = 40$ MeV).

We are taking noninteracting nuclear matter with density $n = 1.5n_0$ for the mantle of our “stars”. In the case of neutral unpaired quark matter in weak equilibrium, the sum on i runs over the nine quarks and the Fermi momenta are independent of color and are given by [30]

$$\begin{aligned} p_F^d &= \mu + \frac{M_s^2}{12\mu} \\ p_F^u &= \mu - \frac{M_s^2}{6\mu} \\ p_F^s &= \mu - \frac{5M_s^2}{12\mu}, \end{aligned} \quad (42)$$

up to corrections of order M_s^4/μ^3 . We are using matter with $\mu = 500$ MeV in the core of our “stars”.

Fig. 3 shows the cooling curves obtained by solving (39) for the four toy stars we have described, plotted on a log-log plot. Each curve has an early time power law during the period when cooling by neutrino emission dominates, namely the first 10^5 or so years. At early times, $L_\gamma \ll L_\nu$ because $L_\gamma \sim R^2$ whereas $L_\nu \sim R^3$. Because L_ν drops much more rapidly than L_γ as T decreases, at late times L_γ dominates and a new power law is seen.

It is easy to see why power law solutions arise. In any temperature regime in which the numerator and the denominator of the right hand side of (39) are each dominated by one of their component terms, the cooling equa-

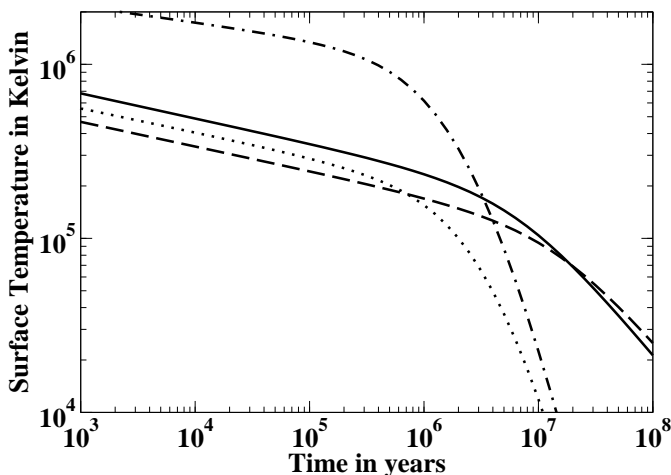


FIG. 4: Same as Fig. 3, except that here we plot T_{surface} , related to the interior temperatures plotted in Fig. 3 by Eq. (36).

tion takes the form

$$\frac{dT}{dt} = -aT^p \quad (43)$$

for some p and a . For example, for a star that is made entirely of nuclear matter, during the epoch when $L_\nu \gg L_\gamma$ we have $p = 7$, coming from $L_\nu \sim T^8$ and $c_V^{nm} \sim T$. For $p > 1$, (43) has a power-law solution

$$T = [a(p-1)t]^{-\frac{1}{p-1}}. \quad (44)$$

There are no arbitrary constants in this solution. We initialize the differential equation with some temperature T_0 at a time $t_0 = 1$ year, chosen because by that time the interior star can reasonably be treated as isothermal. The initial condition $T_0(t_0)$ does not appear in the power law solution: it only affects how the power law solution is reached, if $T_0(t_0)$ does not lie on it. Once the power law solution is reached, the form of the solution to the differential equation is independent of the initial condition. We begin all our plots at $t = 1000$ years, by which time the solution is on the power law (44) for any reasonable choice of $T_0(t_0)$.

During the epoch when $L_\nu \gg L_\gamma$, a star made entirely of nuclear matter has $p = 7$ and $T \sim t^{-1/6}$. For the stars with unpaired quark matter, or gCFL quark matter, $p = 5$ and $T \sim t^{-1/4}$ during this epoch. This explains how similar the three quark matter core curves are during the first 10^5 years, and why all three stars with quark matter cores are colder than the nuclear matter star. Note that the gCFL quark matter has $L_\nu \sim T^{5.5}$ and $c_V \sim T^{0.5}$, both enhanced by $1/T^{0.5}$ relative to that of unpaired quark matter, and indeed relative to any phase of nuclear or quark matter in which direct Urca processes

occur that has been considered previously. But, the effect of these enhancements cancel in the cooling curve during the epoch when $L_\nu \gg L_\gamma$. There are now a number of indications [43] that some neutron stars with ages of order 10^3 to 10^5 years (presumably the heavier ones, although this is certainly not demonstrated) are significantly colder than would be expected in the absence of direct Urca neutrino emission, whereas other (presumably less massive) stars have temperatures consistent with theoretical cooling curves calculated upon assuming nuclear matter composition. Were this to be confirmed, the discovery of direct Urca emission with $T \sim t^{-1/4}$, instead of the slower $T \sim t^{-1/6}$, could indicate the presence of any number of dense matter phases, including gCFL quark matter but also including nuclear matter leavened with either hyperons, kaons or pions.

At late times, when $L_\gamma \gg L_\nu$ all stars except those containing gCFL quark matter have $p = 2.2 - 1 = 1.2$ because $L_\gamma \sim T^{2.2}$ and $c_V \sim T$, and hence cool with $T \sim t^{-1/0.2} = t^{-5}$. This explains the rapidly dropping temperatures at late times for the stars without gCFL quark matter in Fig. 3. If the volume of gCFL matter is sufficient (more on this below) it dominates the heat capacity of the star, yielding $p = 2.2 - 0.5 = 1.7$ because $c_V \sim T^{0.5}$, and hence the star cools with $T \sim t^{-1/0.7} = t^{-1.4}$ at late times. The gCFL matter keeps the aging star warm by virtue of its large heat capacity. Hence, the title of our paper.

We show the surface temperatures of our toy stars in Fig. 4. It is tempting to put data obtained from the observation of real stars on this plot, but we resist the temptation given that our “stars” are not realistic. The qualitative impact of gCFL quark matter is, however, clear: stars which are old enough that they cool by photon emission stay much warmer if they contain a gCFL hot water bottle. In our Fig. 4, which should be taken as illustrative and not yet as a quantitative prediction, the effect is a full order of magnitude for 10^7 -year old stars, and gets much larger for older stars, as the cooling curves of all stars except those containing gCFL quark matter drop rapidly.

In Fig. 5, we investigate the dependence of the cooling curves on the volume of gCFL quark matter present in the core of the star. We see that the “hot water bottle effect” is present for $R_{\text{core}} = 3$ km, but reduced in magnitude. For $R_{\text{core}} = 1$ km, no effect is visible: the effect does occur, but only at even lower temperatures than we have plotted. (Because its heat capacity is $c_V \sim T^{0.5}$, if any gCFL quark matter is present it will eventually dominate the heat capacity of the entire star, no matter how small its volume fraction. For $R_{\text{core}} = 1$ km, this occurs at temperatures below those we have plotted.) Note that what we are referring to as $R_{\text{core}} = 5$ km could equally well describe a star with a shell of gCFL quark matter extending between radii of 4.5 and 6 km.

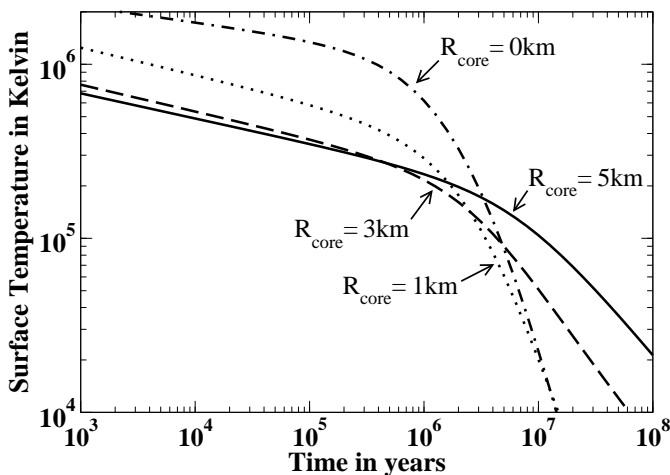


FIG. 5: Cooling curves showing the surface temperature of stars with gCFL cores with $\Delta_0 = 25$ MeV for $R_{\text{core}} = 5$ km (solid; same as solid curve in Fig. 4), $R_{\text{core}} = 3$ km (dashed), $R_{\text{core}} = 1$ km (dotted), $R_{\text{core}} = 0$ km (dot-dashed; same as dot-dashed curve in Fig. 4).

VI. OUTLOOK

We hope that our results challenge observers to constrain the temperature of neutron stars that are 10 million years old or older. Prior to our work, all proposed cooling curves for these old stars drop so fast into unobservability that there has been little motivation to make the effort to obtain the best constraints possible on their temperatures. Given that we know of isolated neutron stars that are younger than a million years old and closer than 200 parsecs, it is reasonable to expect that there are 10^7 -year old isolated neutron stars closer than 100 parsecs to earth. At first we were concerned that if such old nearby stars had temperatures of order 10^5 K, as Fig. 4 suggests will be the case if they contain gCFL hot water bottles, they should already have been detected. However, initial estimates suggest that they will in fact be quite a challenge to find, since the peak of a 10^5 K black body spectrum lies in the far ultraviolet, where the interstellar medium is opaque, and since they will be quite faint in the accessible UV and visible wavelengths [44]. Another option, perhaps easier than finding these stars without knowing where to look, is to study nearby old pulsars, already detected by their nonthermal emission, and to constrain their thermal emission hence putting an upper bound on their temperature. This has been done for PSR 0950+08, whose spin-down age is $10^{7.2}$ years, yielding the bound $T < 10^{5.2}$ K [45]. This limit is quite promising, as it is close to the curves in Fig. 4 describing

the cooling of our toy star with a gCFL core. And, we are confident that we have not thought of the best way of looking for aging but still warm neutron stars. We are therefore hopeful that the opportunity to make an unambiguous discovery of the presence of quark matter within neutron stars or to rule out the presence of gCFL quark matter in the entire region of the QCD phase diagram sampled by neutron stars will stimulate observers to rise to the challenge.

Much theoretical work remains to be done. Interesting microphysical questions about the gCFL phase remain, and have been enumerated in Refs. [4, 6]. Phases with some features in common with the gCFL phase can be unstable with respect to inhomogeneous mixed phases [46], and although the gCFL phase is stable with respect to all straightforward mixed phase possibilities [4, 47], an exhaustive investigation has not yet been performed. Perhaps the most interesting open questions are the possibilities of K^0 -condensation [36, 37] or gluon condensation [48] in the gCFL phase. Either could change our quantitative results for its c_V and ε_ν , but neither is likely to change their unusual T -dependence: $c_V \sim T^{0.5}$ and $\varepsilon_\nu \sim T^{5.5}$. (Neither K^0 -mesons nor gluons [30, 32] would affect the \tilde{Q} -charge balance, which is responsible for the existence of the gapless quasiparticle with a quadratic dispersion relation in Fig. 1, whose consequence in turn is the unusual T -dependence of the gCFL c_V and ε_ν .) As far as theoretical astrophysical work, our results for c_V and ε_ν must be incorporated into calculations of cooling curves for stars with realistic atmospheres and density profiles before plots like those in Figs. 4 and 5 can be compared quantitatively to data. Nonetheless, our conclusion that gCFL quark matter within a neutron star will keep the star warm in its old age relies only on the unusual T -dependence of the gCFL specific heat, and is therefore expected to be robust.

Acknowledgments

We thank David L. Kaplan for orientation on various questions related to observations and Kenji Fukushima for assistance with quasiparticle dispersion relations, and acknowledge helpful conversations with them and with Michael Forbes. We thank Igor Shovkovy for finding an error in a previous version of this paper. PJ is grateful to the Research Science Institute of the Center for Excellence in Education for supporting her research. This research was supported in part by DOE grants DE-FG02-91ER40628, DF-FC02-94ER40818, and DE-FG02-93ER40762.

[1] For reviews, see K. Rajagopal and F. Wilczek, arXiv:hep-ph/0011333; M. G. Alford, Ann. Rev. Nucl. Part. Sci. **51**, 131 (2001) [arXiv:hep-ph/0102047];

G. Nardulli, Riv. Nuovo Cim. **25N3**, 1 (2002) [arXiv:hep-ph/0202037]; S. Reddy, Acta Phys. Polon. B **33**, 4101 (2002) [arXiv:nucl-th/0211045];

- T. Schäfer, arXiv:hep-ph/0304281; M. Alford, arXiv:nucl-th/0312007.
- [2] M. G. Alford, K. Rajagopal and F. Wilczek, Nucl. Phys. B **537**, 443 (1999) [arXiv:hep-ph/9804403].
- [3] M. Alford, C. Kouvaris and K. Rajagopal, Phys. Rev. Lett. **92**, 222001 (2004) [arXiv:hep-ph/0311286].
- [4] M. Alford, C. Kouvaris and K. Rajagopal, Phys. Rev. D., to appear [arXiv:hep-ph/0406137].
- [5] S. B. Ruster, I. A. Shovkovy and D. H. Rischke, Nucl. Phys. A **743**, 127 (2004) [arXiv:hep-ph/0405170].
- [6] K. Fukushima, C. Kouvaris and K. Rajagopal, arXiv:hep-ph/0408322.
- [7] J. M. Lattimer and M. Prakash, Science **304**, 536, (2004) [arXiv:astro-ph/0405262].
- [8] M. Alford, M. Braby, M. Paris and S. Reddy, arXiv:nucl-th/0411016.
- [9] M. Burgay *et al.*, Nature **426**, 531 (2003); A. G. Lyne *et al.*, Science **303**, 1153 (2004).
- [10] M. Kramer *et al.*, arXiv:astro-ph/0405179; I. A. Morrison, T. W. Baumgarte, S. L. Shapiro and V. R. Pandharipande, arXiv:astro-ph/0411353; J. M. Lattimer and B. F. Schutz, arXiv:astro-ph/0411470.
- [11] M. G. Alford, K. Rajagopal, S. Reddy and F. Wilczek, Phys. Rev. D **64**, 074017 (2001) [arXiv:hep-ph/0105009].
- [12] N. K. Glendenning, S. Pei and F. Weber, Phys. Rev. Lett. **79**, 1603 (1997) [arXiv:astro-ph/9705235].
- [13] N. K. Glendenning and F. Weber, Astrophys. J. **559**, L119 (2001) [arXiv:astro-ph/0003426].
- [14] D. Chakrabarty *et al.*, Nature **424**, 42 (2003); R. Wijnands *et al.*, Nature **424**, 44 (2003); D. Chakrabarty, arXiv:astro-ph/0408004.
- [15] J. Madsen, Phys. Rev. Lett. **85**, 10 (2000) [arXiv:astro-ph/9912418].
- [16] C. Manuel, A. Dobado and F. J. Llanes-Estrada, arXiv:hep-ph/0406058.
- [17] M. G. Alford, J. A. Bowers and K. Rajagopal, Phys. Rev. D **63**, 074016 (2001) [arXiv:hep-ph/0008208]; J. A. Bowers, J. Kundu, K. Rajagopal and E. Shuster, Phys. Rev. D **64**, 014024 (2001) [arXiv:hep-ph/0101067]; J. Kundu and K. Rajagopal, Phys. Rev. D **65**, 094022 (2002) [arXiv:hep-ph/0112206]; J. A. Bowers and K. Rajagopal, Phys. Rev. D **66**, 065002 (2002) [arXiv:hep-ph/0204079]; R. Casalbuoni and G. Nardulli, Rev. Mod. Phys. **263**, 320 (2004) [arXiv:hep-ph/0305069]. R. Casalbuoni, M. Ciminale, M. Mannarelli, G. Nardulli, M. Ruggieri and R. Gatto, arXiv:hep-ph/0404090.
- [18] G. W. Carter and S. Reddy, Phys. Rev. D **62**, 103002 (2000) [arXiv:hep-ph/0005228]; S. Reddy, M. Sadzikowski and M. Tachibana, Nucl. Phys. A **714**, 337 (2003) [arXiv:nucl-th/0203011]; S. Reddy, M. Sadzikowski and M. Tachibana, Phys. Rev. D **68**, 053010 (2003) [arXiv:nucl-th/0306015]; J. Kundu and S. Reddy, arXiv:nucl-th/0405055.
- [19] P. Jaikumar, M. Prakash and T. Schafer, Phys. Rev. D **66**, 063003 (2002) [arXiv:astro-ph/0203088].
- [20] G. Baym and C. J. Pethick, Ann. Rev. Astron. Astrophys. **17**, 415 (1979); C. J. Pethick, Rev. Mod. Phys., **64**, 1133 (1992); M. Prakash, in Nuclear and Particle Astrophysics, eds. J. G. Hirsch and D. Page, 153 (Cambridge: Cambridge University Press, 1998); D. G. Yakovlev, A. D. Kaminker, O. Y. Gnedin and P. Haensel, Phys. Rept. **354**, 1 (2001) [arXiv:astro-ph/0012122]; D. G. Yakovlev and C. J. Pethick, Ann. Rev. Astron. Astrophys. **42**, 169 (2004).
- [21] S. L. Shapiro and S. A. Teukolsky, **Black Holes, White Dwarfs and Neutron Stars**, (New York: Wiley, 1983).
- [22] D. Page, M. Prakash, J. M. Lattimer and A. Steiner, Phys. Rev. Lett. **85**, 2048 (2000) [arXiv:hep-ph/0005094].
- [23] D. Page, J. M. Lattimer, M. Prakash and A. W. Steiner, arXiv:astro-ph/0403657.
- [24] D. G. Yakovlev, O. Y. Gnedin, M. E. Gusakov, A. D. Kaminker, K. P. Levenfish and A. Y. Potekhin, arXiv:astro-ph/0409751.
- [25] N. K. Glendenning, Astrophys. J., **293**, 470 (1985).
- [26] J. N. Bahcall and R. A. Wolf, Phys. Rev. B **140**, 1452 (1965).
- [27] D. B. Kaplan and A. E. Nelson, Phys. Lett. B **175**, 57 (1986); D. B. Kaplan and A. E. Nelson, Phys. Lett. B **179**, 409E (1986)
- [28] N. Iwamoto, Phys. Rev. Lett. **44**, 1637 (1980); N. Iwamoto, Annals Phys. **141**, 1 (1982)
- [29] I. A. Shovkovy and P. J. Ellis, Phys. Rev. C **66**, 015802 (2002) [arXiv:hep-ph/0204132].
- [30] M. Alford and K. Rajagopal, JHEP **0206**, 031 (2002) [arXiv:hep-ph/0204001];
- [31] K. Iida and G. Baym, Phys. Rev. D **63**, 074018 (2001) [hep-ph/0011229]; A. W. Steiner, S. Reddy and M. Prakash, Phys. Rev. D **66**, 094007 (2002) [arXiv:hep-ph/0205201]; F. Neumann, M. Buballa and M. Oertel, Nucl. Phys. A **714**, 481 (2003) [arXiv:hep-ph/0210078]; A. Gerhold and A. Rebhan, Phys. Rev. D **68**, 011502 (2003) [arXiv:hep-ph/0305108]; A. Kryjevski, Phys. Rev. D **68**, 074008 (2003) [arXiv:hep-ph/0305173]; D. D. Dietrich and D. H. Rischke, Prog. Part. Nucl. Phys. **53**, 305 (2004) [arXiv:nucl-th/0312044].
- [32] A. Gerhold, arXiv:hep-ph/0411086.
- [33] K. Rajagopal and F. Wilczek, Phys. Rev. Lett. **86**, 3492 (2001) [arXiv:hep-ph/0012039].
- [34] W. V. Liu, F. Wilczek and P. Zoller, arXiv:cond-mat/0404478.
- [35] P. F. Bedaque and T. Schafer, Nucl. Phys. A **697**, 802 (2002) [arXiv:hep-ph/0105150]; D. B. Kaplan and S. Reddy, Phys. Rev. D **65**, 054042 (2002) [arXiv:hep-ph/0107265]; A. Kryjevski, D. B. Kaplan and T. Schafer, arXiv:hep-ph/0404290; M. Buballa, arXiv:hep-ph/0410397.
- [36] M. M. Forbes, arXiv:hep-ph/0411001.
- [37] A. Kryjevski and T. Schaefer, arXiv:hep-ph/0407329; A. Kryjevski and D. Yamada, arXiv:hep-ph/0407350.
- [38] I. Shovkovy and M. Huang, Phys. Lett. B **564**, 205 (2003); E. Gubankova, W. V. Liu and F. Wilczek, Phys. Rev. Lett. **91**, 032001 (2003) [arXiv:hep-ph/0304016]; M. Huang and I. Shovkovy, arXiv:hep-ph/0307273.
- [39] M. G. Alford, J. Berges and K. Rajagopal, Phys. Rev. Lett. **84**, 598 (2000) [arXiv:hep-ph/9908235].
- [40] A. Ipp, A. Gerhold and A. Rebhan, Phys. Rev. D **69**, 011901 (2004) [arXiv:hep-ph/0309019]; A. Gerhold, A. Ipp and A. Rebhan, arXiv:hep-ph/0406087.
- [41] T. Schafer and K. Schwenzer, arXiv:astro-ph/0410395.
- [42] E. H. Gundmundsson, C. J. Pethick and R. I. Epstein, Astrophys. J. **259**, L19 (1982); E. H. Gundmundsson, C. J. Pethick and R. I. Epstein, Astrophys. J. **272**, 286 (1983).
- [43] P. Slane, D. J. Helfand and S. S. Murray, Astrophys. J. **571**, L45 (2002) [arXiv:astro-ph/0204151]; D. L. Kaplan *et al.*, Astrophys. J. Supp. **153**, 269 (2004)

- [arXiv:astro-ph/0403313]; J. P. Halpern, E. V. Gotthelf, F. Camilo, D. J. Helfand and S. M. Ransom, *Astrophys. J.* **612**, 398 (2004) [astro-ph/0404312].
- [44] D. L. Kaplan, private communication.
- [45] V. E. Zavlin and G. G. Pavlov, *Astrophys. J.* **616**, 452 (2004) [arXiv:astro-ph/0405212]. See D. Page, *Astrophys. J.* **479**, L43 (1997) and Ref. [22] for an attempt to obtain such a limit using older data.
- [46] P. F. Bedaque, *Nucl. Phys. A* **697**, 569 (2002) [arXiv:hep-ph/9910247]; P. F. Bedaque, H. Caldas and G. Rupak, *Phys. Rev. Lett.* **91**, 247002 (2003) [arXiv:cond-mat/0306694]; H. Caldas, *Phys. Rev. A* **69**, 063602 (2004) [arXiv:hep-ph/0312275]; M. M. Forbes, E. Gubankova, W. V. Liu and F. Wilczek, arXiv:hep-ph/0405059; S. Reddy and G. Rupak, arXiv:nucl-th/0405054.
- [47] M. Alford, C. Kouvaris and K. Rajagopal, arXiv:hep-ph/0407257.
- [48] M. Huang and I. A. Shovkovy, *Phys. Rev. D* **70**, 051501R (2004) [arXiv:hep-ph/0407049]; M. Huang and I. A. Shovkovy, *Phys. Rev. D* **70**, 094030 (2004) [arXiv:hep-ph/0408268]; R. Casalbuoni, R. Gatto, M. Mannarelli, G. Nardulli and M. Ruggieri, *Phys. Lett. B* **605**, 362 (2005) [arXiv:hep-ph/0410401]; I. Gianakakis and H. C. Ren, *Phys. Lett. B* **611**, 137 (2005) [arXiv:hep-ph/0412015]; M. Alford and Q. h. Wang, arXiv:hep-ph/0501078.